1.0 ||||| 2.8 2.
1.1 ||||| 3.2 2.2
3.6 2.0
1.25 ||||| 1.4 ||||| 1.6 1.8
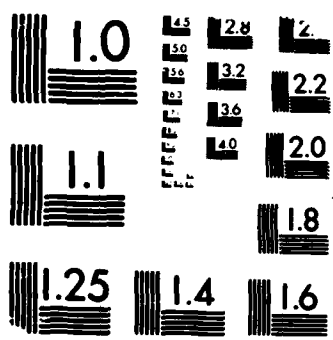
MICROCOPY RESOLUTION TEST CHART
NATIONAL BUREAU OF STANDARDS-1963-A

REPORT DOCUMENTATION PAGE

AD-A191 322

DTIC ELECTE FEB 2 4 1988 D

1b. RESTRICTIVE MARKINGS
NA

3. DISTRIBUTION / AVAILABILITY OF REPORT
Distribution Unlimited; Approved for Public Release

2b. DECLASSIFICATION / DOWNGRADING SCHEDULE
NA

4. PERFORMING ORGANIZATION REPORT NUMBER(S)	MONITORING ORGANIZATION REPORT NUMBER(S)
INDU/DC/GMH/TR-88-17	NA

6a. NAME OF PERFORMING ORGANIZATION	6b. OFFICE SYMBOL (If applicable) NA	7a. NAME OF MONITORING ORGANIZATION
Indiana University		ONR

6c. ADDRESS (City, State, and ZIP Code)	7b. ADDRESS (City, State, and ZIP Code)
Department of Chemistry Bloomington, IN 47405	800 N. Quincy Street Arlington, VA 22217

8a. NAME OF FUNDING / SPONSORING ORGANIZATION	8b OFFICE SYMBOL (If applicable)	9 PROCUREMENT INSTRUMENT IDENTIFICATION NUMBER
		Contract N00014-86-K-0366

8c. ADDRESS (City, State, and ZIP Code)	10. SOURCE OF FUNDING NUMBERS			
	PROGRAM ELEMENT NO.	PROJECT NO.	TASK NO. R&T Code 4134006	WORK UNIT ACCESSION NO

11. TITLE (Include Security Classification)

A New Fiber-Optic-Based Ion Sensor

12 PERSONAL AUTHOR(S)
Frank V. Bright, Greg E. Poirier, and Gary M. Hieftje

13a TYPE OF REPORT	13b TIME COVERED	14. DATE OF REPORT (Year, Month, Day)	15. PAGE COUNT
Technical	FROM ___ TO ___	15 February 1988	30

16. SUPPLEMENTARY NOTATION

To be published in Talanta

17. COSATI CODES			18. SUBJECT TERMS (Continue on reverse if necessary and identify by block number)
FIELD	GROUP	SUB-GROUP	Fiber optics; Sensors; Remote sensing; Ion measurement

19. ABSTRACT (Continue on reverse if necessary and identify by block number)

A fluorimetric fiber-optic-based ion sensor has been developed that employs rhodamine 6G hydrophobically and electrostatically "trapped" on a Nafion film. The sensor is based on the measurement of quenching or enhancement of rhodamine 6G fluorescence by various ions. It was found that ions like Co(II), Cr(III), Fe(II), Fe(III), Cu(II), Ni(II) and NH_4^+ rapidly quench the rhodamine 6G fluorescnece at an initial rate that depends on the ion's concentration. This quenching is then readily reversed by the addition of "reverser" ions like H^+, Li^+, Na^+, K^+, Ba(II), Ca(II), Mn(II), Zn(II) and Mg(II). Again, the initial rate for the attainment of the original fluorescence was found to depend on the reverser ion's concentration. Therefore, by monitoring the quenching directly the concentration of quencher ions can be determined. In addition, by loading the film with quencher and monitoring the initial rate of return toward the original baseline signal one can quantitate non-quenching ions.

20 DISTRIBUTION / AVAILABILITY OF ABSTRACT	21 ABSTRACT SECURITY CLASSIFICATION
☒ UNCLASSIFIED/UNLIMITED ☐ SAME AS RPT ☐ DTIC USERS	Distribution Unlimited

22a NAME OF RESPONSIBLE INDIVIDUAL	22b. TELEPHONE (Include Area Code)	22c. OFFICE SYMBOL
Gary M. Hieftje	(812) 335-2189	

DD FORM 1473, 84 MAR 83 APR edition may be used until exhausted. All other editions are obsolete. SECURITY CLASSIFICATION OF THIS PAGE

UNCLASSIFIED

A NEW FIBER-OPTIC-BASED ION SENSOR

by

Frank V. Bright, Greg E. Poirier, and Gary M. Hieftje

Prepared for Publication

in

TALANTA

Indiana University
Department of Chemistry
Bloomington, Indiana 47405

15 February 1988

88 2

ABSTRACT

A fluorimetric fiber-optic-based ion sensor has been developed that employs rhodamine 6G hydrophobically and electrostatically "trapped" on a Nafion film. The sensor is based on the measurement of quenching or enhancement of rhodamine 6G fluorescence by various ions. It was found that ions like Co(II), Cr(III), Fe(II), Fe(III), Cu(II), Ni(II) and NH_4^+ rapidly quench the rhodamine 6G fluorescnece at an initial rate that depends on the ion's concentration. This quenching is then readily reversed by the addition of "reverser" ions like H^+, Li^+, Na^+, K^+, Ba(II), Ca(II), Mn(II), Zn(II) and Mg(II). Again, the initial rate for the attainment of the original fluorescence was found to depend on the reverser ion's concentration. Therefore, by monitoring the quenching directly the concentration of quencher ions can be determined. In addition, by loading the film with quencher and monitoring the initial rate of return toward the original baseline signal one can quantitate non-quenching ions.

INTRODUCTION

The area of fiber-optic sensors has bloomed over the past five years. The recent advances and trends in fiber-optic sensors have been described in several excellent reviews (1-10). Assuredly, most of the interest in fiber-optic sensors arises not only from the ability to qualitatively identify and quantitatively determine chemical species, but also from the power of carrying out these tasks remotely. One of the stumbling blocks in the development of effective sensors has been the identification of immobilized reagent phases which are suitable for the target analyte(s) while yet
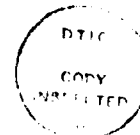
For

on

Availability Codes

| | Avail and/or |
| Dist | Special |

A-1

exhibiting adequate sensitivity. Ideally, these immobilized reagents should also have reversible behavior and be very durable.

Narayanaswamy and Serilla (11) have developed a reflectance-based sensor for the determination of sulphide ion which has detection limits in the m$\underline{M}$ range. Other reflectance-based sensors have also been developed for pH (12), ammonia (13), and moisture (14). In addition to these reflectance approaches, fluorimetric-based sensors have been described for O_2 (15) and for halide ions (16,17). Saari and Seitz have developed a complexometric sensor for the determination of Be(II) that employs immobilized morin (18) and offers detection limits in the $\mu\underline{M}$ range. The same authors applied this sensor to the determination of Al(III) and again obtained detection limits on the $\mu\underline{M}$ level (19). However, they noted interferences from Co(II), Mg(II), Cu(II), and Fe(III). Zhujun and Seitz have described a complexometric fluorescence-based sensor which utilizes 5-sulfo-8-hydroxyquinoline for the determination of Al(III), Mg(II), Zn(II), Cd(II), Ca(II), Be(II), and Sr(II) (20). Detection limits were again of the order of $\mu\underline{M}$. Unfortunately, the spectral character of the complexes was such that mixtures could not be resolved although it was proposed that derivative spectroscopy might be employed for this resolution. Recently, Seitz and coworkers have described a selective complexometric sensor for the determination of Na^+ that offers detection limits of 20 m$\underline{M}$ (20). This sensor employed 8-anilino-1-naphthalenesulfonic acid, Cu(II)-polyethyleneimine and a commercial sodium-selective ionophore immobilized on silica (21). In this case selectivity was provided by the selective ionophore.

In the present paper we describe a new fluorimetric fiber-optic sensor for the determination of several ionic species. The sensor employs as the reagent phase a fluorophore trapped on a Nafion film. To our knowledge,

this is the first application of Nafion-trapped species to fiber-optic sensing. Nafion is a perfluorinated poly-sulfate polymer. It has been proposed (22) that "ionopores" are formed within Nafion as the solvent evaporates and the charged sulfate groups agglomerate in the developing film. These pores act as cation-selective "holes" in the Nafion membrane. Cationic dye molecules can then reside on the Nafion membrane with their organic portions hydrophobically bound to the bulk membrane while their charged groups reside in the ionopore.

Immobilization on Nafion is especially attractive for rhodamine 6G because it is both electrostatically and hydrophobically bound to the Nafion polyanion in aqueous solution. Furthermore, because of the anionic character of Nafion, positively charged ions are preferentially permitted to approach the fluorophore, so anionic interferences are minimal. In addition, Nafion-immobilized fluorimetric fiber-optic sensors can be fashioned simply, rapidly, and are quite durable.

In this study ionic species like Co(II), Cr(III), Fe(III), Cu(II), Fe(II), Ni(II) and NH_4^+ were found to enter the ionopores and to quench the immobilized rhodamine 6G fluorescence. This is not too unlike the effects observed previously for rhodamine dyes in bulk solution (23). In contrast, ions like H^+, K^+, Li^+, Na^+, Ba(II), Ca(II), Mn(II), Zn(II) and Mg(II) did not quench the rhodamine 6G fluorescence. However, these latter ions served as "reversers" in that they displaced the quencher ions and helped to reestablish the original level of rhodamine 6G fluorescence. The reversers can then easily be quantitated by monitoring the initial rate of fluorescence increase after the film has been loaded with a quencher ion.

THEORY

Fluorescence from the Nafion/rhodamine 6G sensor is quenched, as described above, by various positive ions. In the case of the reverser ions, a competition occurs for ionophoric sites occupied by the quenching ions; reverser ions can kinetically displace the quenchers and thereby regenerate the original fluorescence signal.

The rate ($d[Q_N]/dt$) at which the quencher diffuses into the Nafion film, reaches the ionophoric sites, and quenches the rhodamine 6G fluorescence is described by the following relation:

$$\frac{d[Q_N]}{dt} = k_1 F[Q_S] \tag{1}$$

where [Q] is the equilibrium quencher concentration, subscripts S and N represent the ions in solution or in the Nafion, respectively, k_1 is the rate coefficient for the "transfer" of the quenching ion from the bulk solution into the Nafion, and F is the fraction of rhodamine-laden ionophoric sites available to the quencher ions. If the observed fluorescence intensity as a function of time (dI/dt) depends on $[Q_N]$ then:

$$\frac{D[Q_N]}{dt} = -k_2 \frac{dI}{dt} \tag{2}$$

where k_2 is a new proportionality constant that incorporates the dependence of $[Q_N]$, F, and k_1 on dI/dt. Upon combination of Equations 1 and 2 the fluorescence intensity can be related to the quencher concentration in the bulk solution ($[Q_S]$) as:

$$\frac{dI}{dt} = -\frac{k_1}{k_2} F[Q_S] \tag{3}$$

At time t=0 the available number of ionophoric sites within the Nafion (F) is constant (for a given Nafion/rhodamine 6G sensor) and $(dI/dt)_{t=0}$ (the initial rate of quenching) is given by:

$$\left(\frac{dI}{dt}\right)_{t=0} = -k[Q_S]_{t=0} \tag{4}$$

where $k=(k_1 F/k_2)$ and $[Q_S]_{t=0}$ is simply the concentration of quencher species in the bulk solution at time zero. In an analogous fashion one arrives at a similar equation for the reverser ion:

$$\left(\frac{dI}{dt}\right)'_{t=0} = k'[R_S]_{t=0} \tag{5}$$

where R denotes a reverser ion. Therefore, a plot of $(dI/dt)_{t=0}$ vs. quencher ion or $(dI/dt)'_{t=0}$ vs. reverser ion will be linear. These linear plots can then be employed as working curves for determinations of either the quencher or reverser ions, respectively.

EXPERIMENTAL

Reagents. Each of the analyte ions was obtained from readily available reagent-grade materials. Initially, the various ions were used as the chloride salts, but later studies confirmed little response dependence on the counter ion. All solutions were prepared in distilled-deionized water. A 0.100 M stock solution of each metal ion was prepared and working solutions prepared by serial dilution. Rhodamine 6G was purchased

commercially (Exciton Co.) and was used as received. Nafion (perfluorinated
ion-exchange powder) was purchased as a 5 wt.% solution in a mixture of
aliphatic alcohols and water (Aldrich; cat. # 27,470-4). Hydrofluoric acid
(70:30 HF:pyridine) was from Aldrich also.

<u>Instrumentation</u>. All UV-visible absorbance spectra were recorded on a
Hewlett-Packard model 8450 diode-array spectrophotometer.

Figure 1 shows a schematic diagram of the fiber-optic-based instrument
used in these studies. The excitation source consists of an intensity-
modulated Xe arc lamp system (Varian EIMAC model PS 300-1 power supply and
model 300-2 lamp unit). Early versions of the instrument employed a cw
argon-ion laser (Spectra Physics model 171), but satisfactory results were
achieved with the Xe arc lamp also. The Xe lamp intensity is modulated by a
square wave from a function generator (Krohn-Hite model 1600 lin/log sweep
generator). For all results presented here, the average lamp current was
17 A (peak current 22 A) at a modulation frequency of 150 Hz.

The excitation wavelength is selected by a 15-nm bandpass filter
centered at 500 nm. The filtered excitation light is then focussed by a
lens (f.l. = 60 mm) into one end of the bifurcated-fiber-optic sensor
(Figure 2). The fiber-optic sensor consists of two identical 2-m segments
of 400 μm-diameter UV-transmitting fiber (General Fiber Optics part
14-400). Similar results were also achieved with 200-μm-diameter UV-grade
fibers from Galileo Fiber Optics. The distal ends of the fibers are epoxied
(Epotek 320) together within a 3-mm-i.d. glass capillary. The glass
capillary extends 1 cm below the terminus of the excitation and emission
fibers, in order to ensure that the entire reagent surface is illuminated by
the exciting light. A microscope cover slip is then glued (Superglue, Inc.)

over the opening of the glass capillary as shown in Figure 2. This cover

slip serves as the "support" for the Nafion/rhodamine 6G membrane.

Fluorescence is collected by the second fiber optic (Em., Figure 2) and

directed to a monochromator (Kratos model GM 100-1) whose bandpass is

centered at 550 nm. The resulting photon flux is detected by a

photomultiplier tube (Hamamatsu model R928) operated at a biasing voltage of

-1000 V dc. The output from the photomultiplier is then sent to a fast

current amplifier (Keithley model 427) which is in turn connected to a lock-

in amplifier (Keithley model 840 Auto Loc). The TTL output from the

function generator serves as the reference for the lock-in amplifier.

The output from the lock-in amplifier is then directed to a computer

(Digital Equipment Co. model MINC 11/23) which collects and analyzes the

data through an interactive BASIC subroutine. The program consists

essentially of two parts: 1) data collection (fluorescence intensity vs.

time) and 2) least-squares fitting of the initial portion of the collected

data set (determination of initial rate).

Fiber Preparation. The Nafion/rhodamine 6G film is immobilized at the

distal end of the optical fiber by means of a variant of the method proposed

by Rubenstein and Bard (22). The microscope cover slip, attached to the

fiber's distal end, is first treated with a 70% solution of HF for 0.5-1

minutes. It is important that HF treatment times of longer than 2 minutes

result in both the dissolving of the support glue and destruction of the

microscope cover slip. This HF etching serves to produce a microrough

surface which helps the Nafion adhere to the microscope cover slip.

The reagent phase is produced by pipetting (Ranin Inc.) between 25 and

50 µL of the Nafion solution onto the microscope cover slip. The solvents

are allowed to evaporate at room temperature over a 1-hour period and the sensor rinsed repeatedly with distilled-deionized water. The Nafion-coated coverslip is then quickly dipped in a 10% ethanolic solution of 1.00 m$\underline{M}$ rhodamine 6G, removed and immersed in distilled-deionized water, allowed to air dry for 10 minutes, and rinsed again with water. For long-term storage, the fiber was immersed in water. This sensor, while simple to produce, is quite durable and produces a reproducible response over a period of several weeks. In addition, the sensor is stable for times of several weeks in both acidic (1 $\underline{M}$ HCl) and basic (1 $\underline{M}$ NH$_4$OH) media. However, the film will separate or peel from the cover slip if the sensor is allowed to dry fully.

General Operation. For initial optimization, the detected fluorescence signal is maximized while the sensor is immersed in a water blank. This optimization usually consists of simply repositioning the excitation fiber with respect to the exciting light or minor readjustment of the lock-in amplifier phase setting. Following this initial optimization the system is stable (long-term-signal drift < 5%) for well over 4 hours.

For all the quencher ions studied the rhodamine 6G fluorescence decreases at a rate that is dependent on the quenching-ion concentration. Unfortunately, the quenching is not reversed simply by placing the sensor back into water, but must be reversed by the use of another ion (H$^+$, Na$^+$ or Li$^+$) to displace the quencher. At first it might seem as if this lack of immediate reversibility is a detriment, but in fact it allows us to determine also those ions which reverse the quenching process.

Let us first consider the case of an ionic species (Co(II), Cr(III), Fe(III), Fe(II), Cu(II), Ni(II), and NH$_4^+$) which quenches the fluorescence. As the quenching metal ion diffuses into the Nafion it reduces the rhodamine

6G fluorescence. The rate of this quenching is dependent on two different parameters: 1) the solution concentration of the quenching ion and 2) the identity of the ion. From the fluorescence intensity vs. time plot the initial rate (V_i) for the quenching process is determined and can be related to the initial concentration of quencher. The original fluorescence intensity can then be restored by immersing the sensor in a solution of one of the reversing ions $(H^+, Na^+$ or $Li^+)$.

To determine the concentration of a reverser ion, the fiber is first immersed in a quenching ion (e.g., Cu(II)) and the fluorescence quenched. The sensor is then removed from this solution, rinsed with water, and placed in an appropriate reversing-ion sample solution. The rate at which the fluorescence returns to its original level is dependent on the same two parameters described above. Consequently, the concentration of the reverser ion can be determined from the initial rate for restoration of fluorescence. By simply repeating the experiment at several reversing ion concentrations a working curve of V_i vs. ion concentration can be constructed.

RESULTS AND DISCUSSION

Quencher Ions. Figure 3 shows a typical time-response trace for the sensor operating in the quencher mode. It is apparent that quenching by 10^{-4}M Cu(II) is very rapid and requires less than one minute to reach a nearly steady-state level. Table I compiles detection limits for all the quencher ions studied. The detection limits were defined as that concentration of metal ion which gave an initial rate of fluorescence decay that produced a signal-to-noise ratio of 2. The signal in this case is V_i, the initial rate of fluorescence decrease caused by the quencher; the noise is the standard

deviation of the steady-state fluorescence measured with the sensor immersed in water. The linear dynamic range for the determination of quencher ions extends more than 4 orders of magnitude. Table II shows the statistical information (slope, intercept, correlation coefficient (r^2), and standard error of estimate) for a least-squares analysis of a working curve for each ion. The detection limits parallel the initial rates of quenching for the quenchers as follows: $Co(II) > Cr(III) > Fe(III) > Cu(II) > NH_4^+ > Fe(II) >$ $Ni(II)$. Because these quenching rates were dependent on the identity of the ionic species we chose to explore this feature in more detail.

Unfortunately, we did not find any physical parameter(s) that correlated well with the initial rate of fluorescence decay caused by the quencher ion. For example, the crystal ionic radii, the approximate effective ionic radii, magnetic moments, and fluorescence lifetimes for each of the ions with the sensor do not correlate with the initial rate. Additionally, energy transfer to the absorption bands of the ions can be ruled out as a major contributor because of the very weak absorbances of all quenching ions near 550 nm (see Figure 4). Rhodamine 6G exhibits an emission spectrum centered at 550 nm with a full width at half maximum of 120 nm. Of the ions studied, Cr(III) would be the most likely to exhibit energy transfer (cf. Figure 4), but no correlation was found between the degree of spectral overlap and initial quenching rates.

Regardless of the mechanism(s) involved in the quenching, it is clear that the quenching-based sensor: 1) is quite rapid, 2) has excellent sensitivity, and 3) is simple to operate. In addition, the required instrumentation is rather simple to set up and not very expensive. Advantageously, interferences from traditional fluorescence quenchers

(halides) is nonexistent because the ionopore of the Nafion film simply does not allow the halide to approach within the rhodamine 6G interaction volume. For example, we found little correlation between counter ion (halide) identity and rate of quenching; Br^- and Cl^- salts gave approximately the same response.

Reverser Ions. Figure 5 shows a typical response curve for a reverser ion. Specifically, in this case 10^{-4} $\underline{M}$ Li^+ is used to reverse the quenching caused by 10^{-5} $\underline{M}$ Cu(II). Table III lists the detection limits calculated in the same way as for quencher ions for each of the reverser ions that were studied. In this mode of operation the linear dynamic range of the sensor is over 4 orders of magnitude. Table IV compiles the statistical information (slope, intercept, correlation coefficient $[r^2]$, and standard error of estimate) for a least-squares analysis of each ion's linear working curve. For completeness, the initial rate of enhancement was studied in more detail in an effort to gain insight into this process.

The initial rates of reversal follow the order (Ba(II) > K(I) > Ca(II) > Na(I) > Mn(II) > Zn(II) > Li(I) > Mg(II)), the same as the trend in both crystal ionic radii and approximate effective ionic radii. Figure 6 shows a plot of initial rate of enhancement vs. crystal ionic radii of those ions (24). This plot was generated for Cs(I), K(I), Na(I), Li(I), Ba(II), Mn(II), Zn(II), and Mg(II) at the 10^{-4} $\underline{M}$ level. Clearly, a linear relationship exists (correlation coefficient - 0.932) between size of the ion and the rate at which it restores the fluorescence intensity of Cu(II)-quenched rhodamine 6G. Figure 7 shows a plot of the initial rate vs. effective ionic radii (25) for all the reverser ions studied. In this case the correlation coefficient is only 0.745. From these data it appears that

the size of the reverser ion plays a critical role in the rate of the enhancement (displacement) process; however, such a trend is not readily apparent for the quencher ions.

CONCLUSION

A new sensor has been described for the determination of several ion species. The sensor is simple, easy to operate, durable, and rapid. Common measurement times are 20 seconds and 70 seconds for quencher and reverser ions, respectively. In addition, precision studies have shown that worst case relative standard deviations are 4.5% for quencher ions and 5.8% for reverser ions. Unfortunately, the sensor is nonselective, but several of the ions have quenching or enhancement rates which differ by 40-50%. For this reason the sensor might be especially useful when applied in a sensor array (26).

ACKNOWLEDGEMENT

LITERATURE CITED

1) Milanovich, F. P. and Hirschfeld, T. Adv. Instrum. (1986), 38, 407.

2) Seitz, W. R. Sensors (1985), 2, 6.

3) Wolfbeis, O. S. Trends Anal. Chem. (1985), 4, 184.

4) Narayanaswamay, R. Anal. Proc. (1985), 22, 204.

5) Edmonds, T. E. and Ross, I. D. Anal. Proc. (1985), 22, 206.

6) Peterson, J. I. and Vurek, G. G. Science (1984), 224, 123.

7) Chabay, I. Anal. Chem. (1982), 54, 1071A.

8) Alder, F. E. Fresenius' Z. Anal. Chem. (1986), 324, 372.

9) Hirschfeld, T. Fresenius' Z. Anal. Chem. (1986), 324, 618.

10) Seitz, W. R. Anal. Chem. (1984), 56, 16A.

11) Narayanaswamy, R. and Serilla, F. Analyst (1986), 111, 1085.

12) Kirkbright, G. F.; Narayanaswamy, R. and Welti, N. A. Analyst (1984),
    109, 1025.

13) Giuliani, J. F.; Wohltjen, H. and Jarvis, N. L. Optics Lett. (1983),
    8, 54.

14) Russell, A. P. and Fletcher, K. S. Anal. Chim. Acta (1985), 170, 209.

15) Wolfbeis, O. S.; Offenbacher, H.; Kroneis, H. and Marsoner, H.
    Mikrochim. Acta (Vienna) (1984), I, 153.

16) Urbano, E.; Offenbacher, H. and Wolfbeis, O. S. Anal. Chem. (1984),
    56, 427.

17) Wyatt, W. A.; Poirier, G. E.; Bright, F. V. and Hieftje, G. M. Anal.
    Chem. (1987), 59, 572.

18) Saari, L. A. and Seitz, W. R. Analyst (1984), 109, 655

19) Saari, L. A. and Seitz, W. R. Anal. Chem. (1983), 55, 667.

20) Zhujun, Z. and Seitz, W. R. Anal. Chim. Acta (1985), 171, 251.

21) Zhujun, Z.; Mullin, J. L. and Seitz, W. R. Anal. Chim. Acta (1986), 184, 251.

22) Rubenstein, I. and Bard, A. J. J. Amer. Chem. Soc. (1980), 102, 6641.

23) "CRC Handbook of Organic Analytical Reagents", K. L. Cheng; K. Uneo and T. Imamura, Eds., CRC Press, Boca Raton, FL (1982), p. 465.

24) "CRC Handbook of Chemistry and Physics", 63rd ed., CRC Press, Boca Raton, FL, p. F165.

25) "Handbook of Analytical Chemistry", L. Meites, Ed., McGraw-Hill, New York, NY (1963) p. 1-7.

26) Carey, W. P.; Beebe, K. R.; Kowalski, B. R.; Illman, D. L. and Hirschfeld, T. Anal. Chem. (1986), 58, 149.

TABLE I

DETECTION LIMITS FOR QUENCHER IONS

Ion	Detection Limit (μM)
Co(II)	0.74
Cr(III)	0.82
Fe(III)	0.80
Cu(II)	1.2
Fe(II)	1.9
Ni(II)	2.1

TABLE II

STATISTICAL INFORMATION FOR QUENCHER-ION LINEAR WORKING CURVES

Ion	Slope	Intercept	R^2	Std. Error of Estimate
Co(II)	3.81	0.12	0.981	0.16
Cr(III)	3.46	0.10	0.976	0.18
Fe(III)	3.14	0.09	0.992	0.09
Cu(II)	2.83	0.08	0.973	0.17
Fe(II)	2.51	0.04	0.991	0.11
Ni(II)	2.10	0.02	0.997	0.13

TABLE III

DETECTION LIMITS FOR REVERSER IONS

Ion	Detection Limit (μM)
Cs(1)	0.74
K(I)	0.82
Na(I)	1.4
Li(I)	1.7
H(I)	0.94
Ba(II)	0.81
Ca(II)	1.2
Mn(II)	1.5
Zn(II)	1.6
Mg(II)	1.8

TABLE IV

STATISTICAL INFORMATION FOR REVERSER-ION LINEAR WORKING CURVES

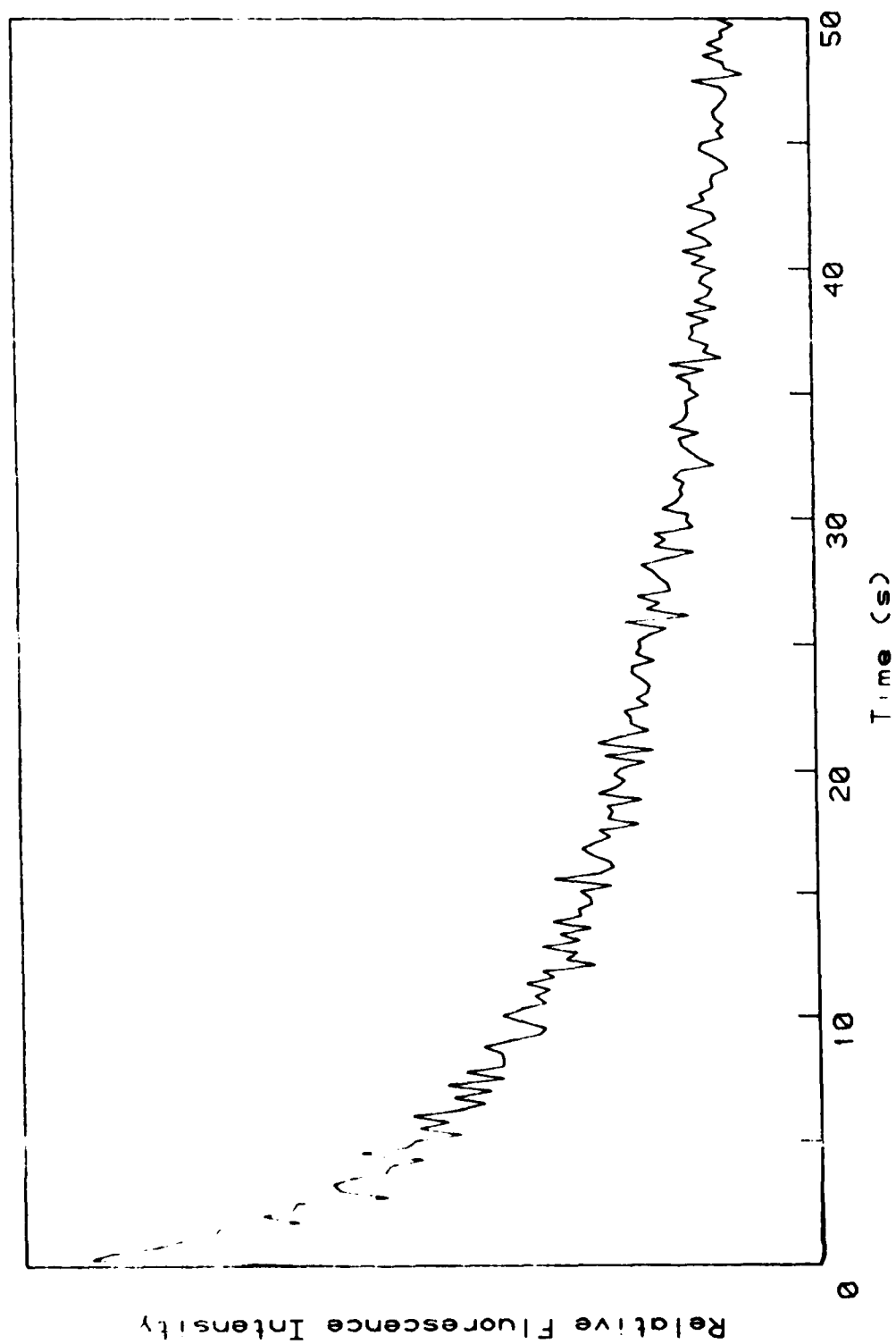| Ion	Slope	Intercept	R^2	Std. Error of Estimate
Cs(I)	3.82	0.13	0.991	0.21
K(I)	3.69	0.14	0.997	0.12
Na(I)	2.73	0.08	0.990	0.13
Li(I)	2.02	-0.02	0.975	0.27
H(I)	3.31	0.16	0.982	0.21
Ba(II)	3.71	0.18	0.952	0.41
Ca(II)	2.93	0.16	0.966	0.42
Mn(II)	2.42	0.01	0.967	0.33
Zn(II)	2.13	0.10	0.983	0.25
Mg(II)	1.81	-0.12	0.976	0.32

FIGURE CAPTIONS

Figure 1.   Schematic diagram of the fiber-optic-based ion-sensing instrument. Mono. – monochromator. Det. – photomultiplier tube detection.

Figure 2.   Schematic diagram of the fiber-optic sensor. Ex. – optical fiber that carries exciting light to the fluorophore. Em. – optical fiber that carries emitted fluorescence radiation from the sensor to the photometric system. Open space indicated between microscope cover slip and fiber optic is an air gap.

Figure 3.   Time dependence of immobilized rhodamine 6G quenching caused by 10^{-4} $\underline{M}$ Cu(II).

Figure 4.   Absorbance spectra of quencher ions at 10^{-2} $\underline{M}$ in aqueous solution.

Figure 5.   Reverser-ion effect for 10^{-4} $\underline{M}$ Li(I); other reverser ions behave similarly. The effect of quenching by 10^{-5} $\underline{M}$ Cu(II) is being reversed.

Figure 6.   Initial slope of the fluorescence intensity vs. time plot (Initial Rate) as a function of the crystal ionic radii of the reverser ions. The quenching from 10^{-5} M Cu(II) is being reversed. Correlation coefficient is 0.932.
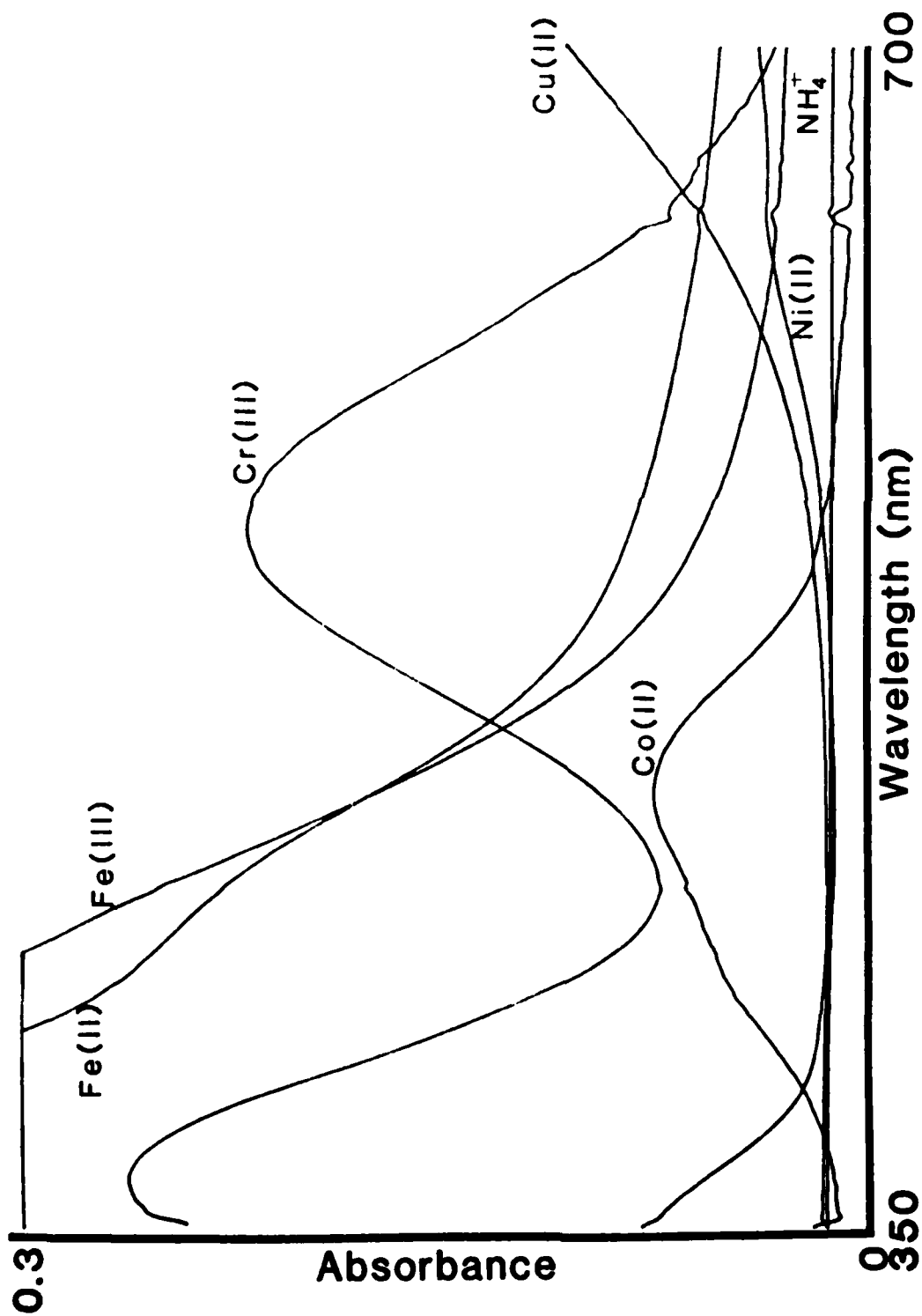
Figure 7.   Initial slope of the fluorescence intensity vs. time plot
             (Initial Rate) as a function of the effective ionic radii of
             the reverser ions.   Correlation coefficient is 0.745. 10^{-5} 1
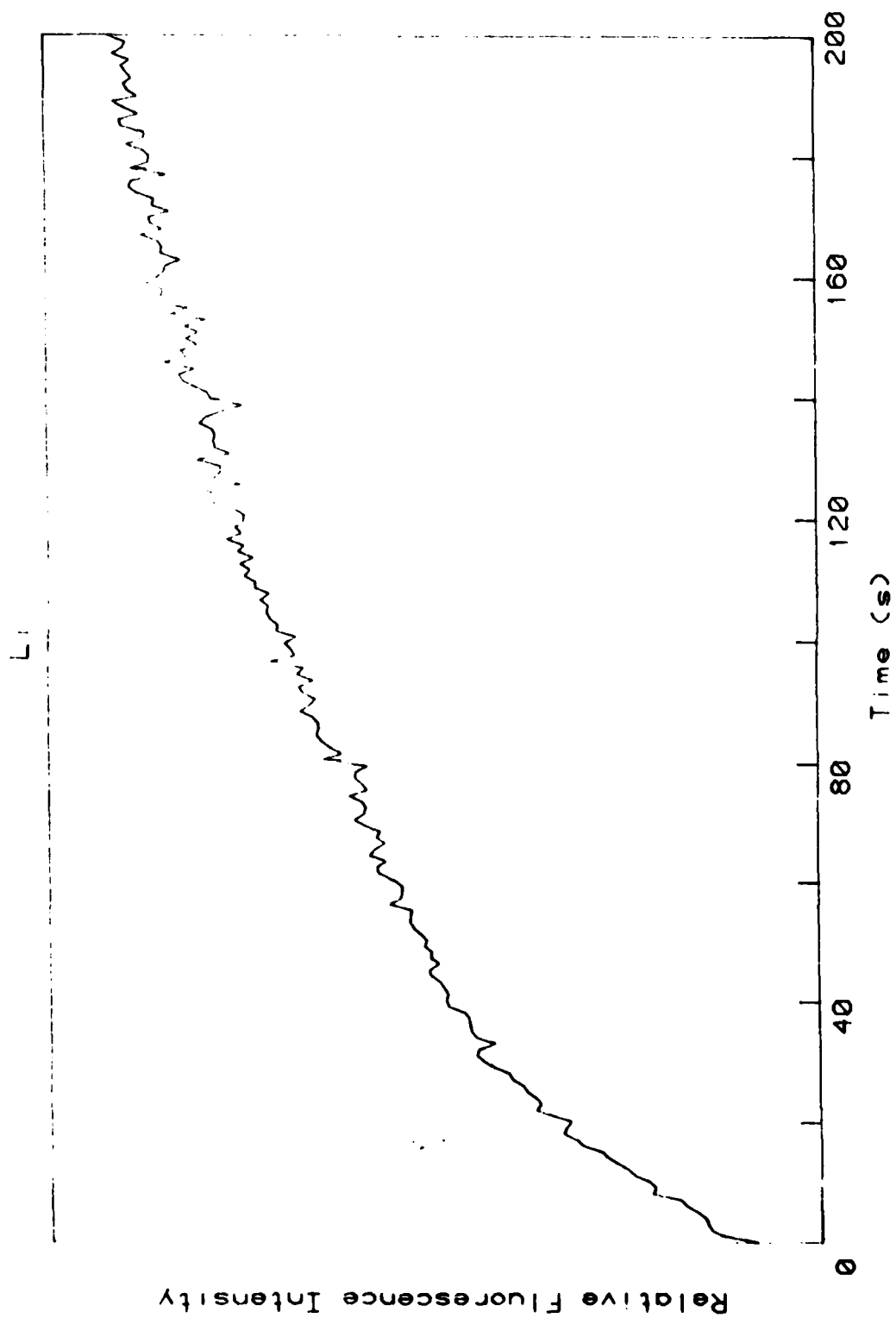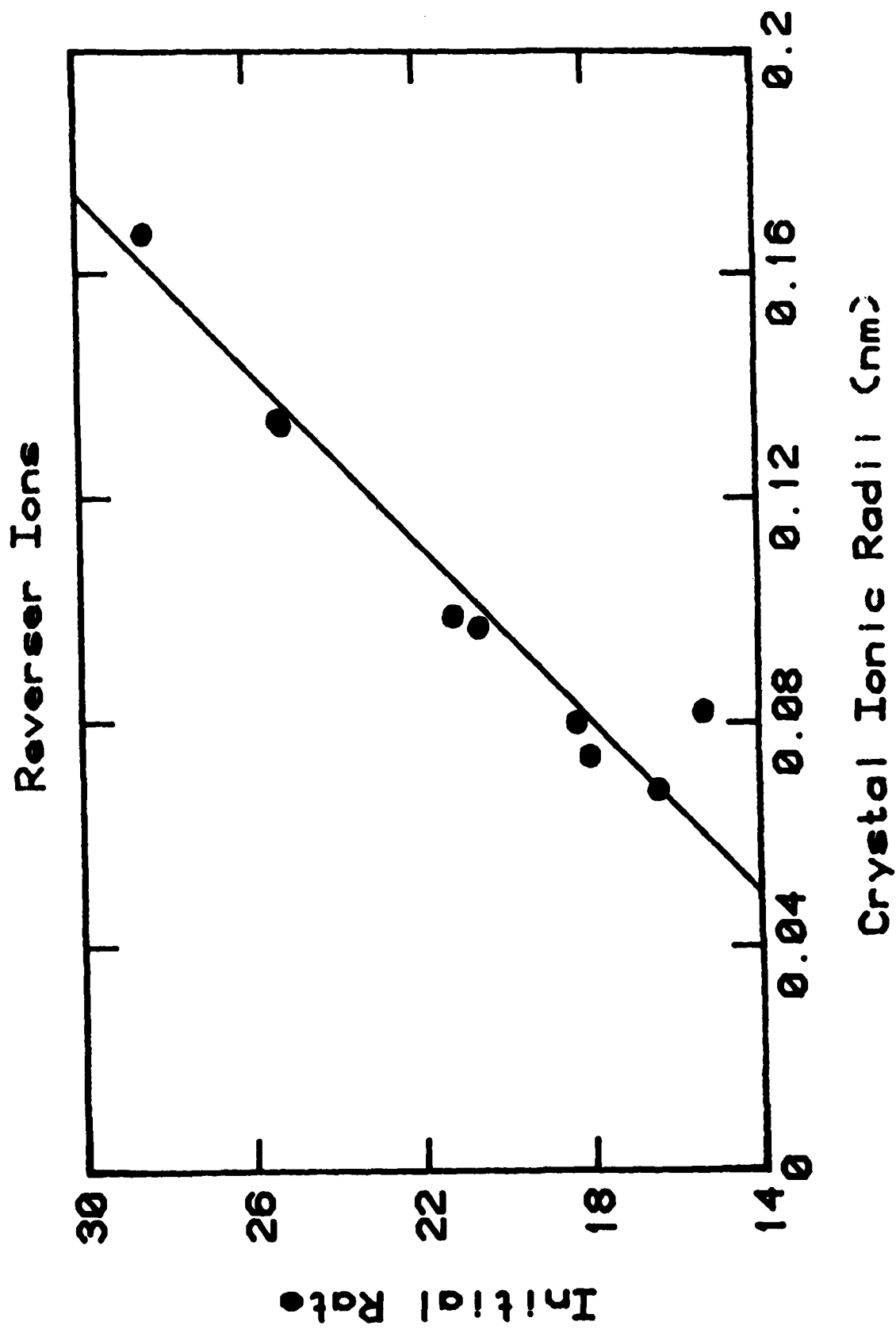   Cu(II) is being reversed.

Fiber Optics

Ex. Em.

Epoxy bond

Glass
Capillary

Microscope
Cover-slip
Support

Nafion & R6G

Cu(II)

Relative Fluorescence Intensity

Time (s)

Relative Fluorescence Intensity

Time (s)

Reverser Ions

Initial Rate

Crystal Ionic Radii (nm)

Reverser Ions

Effective Ionic Radii (nm)

Initial Rate
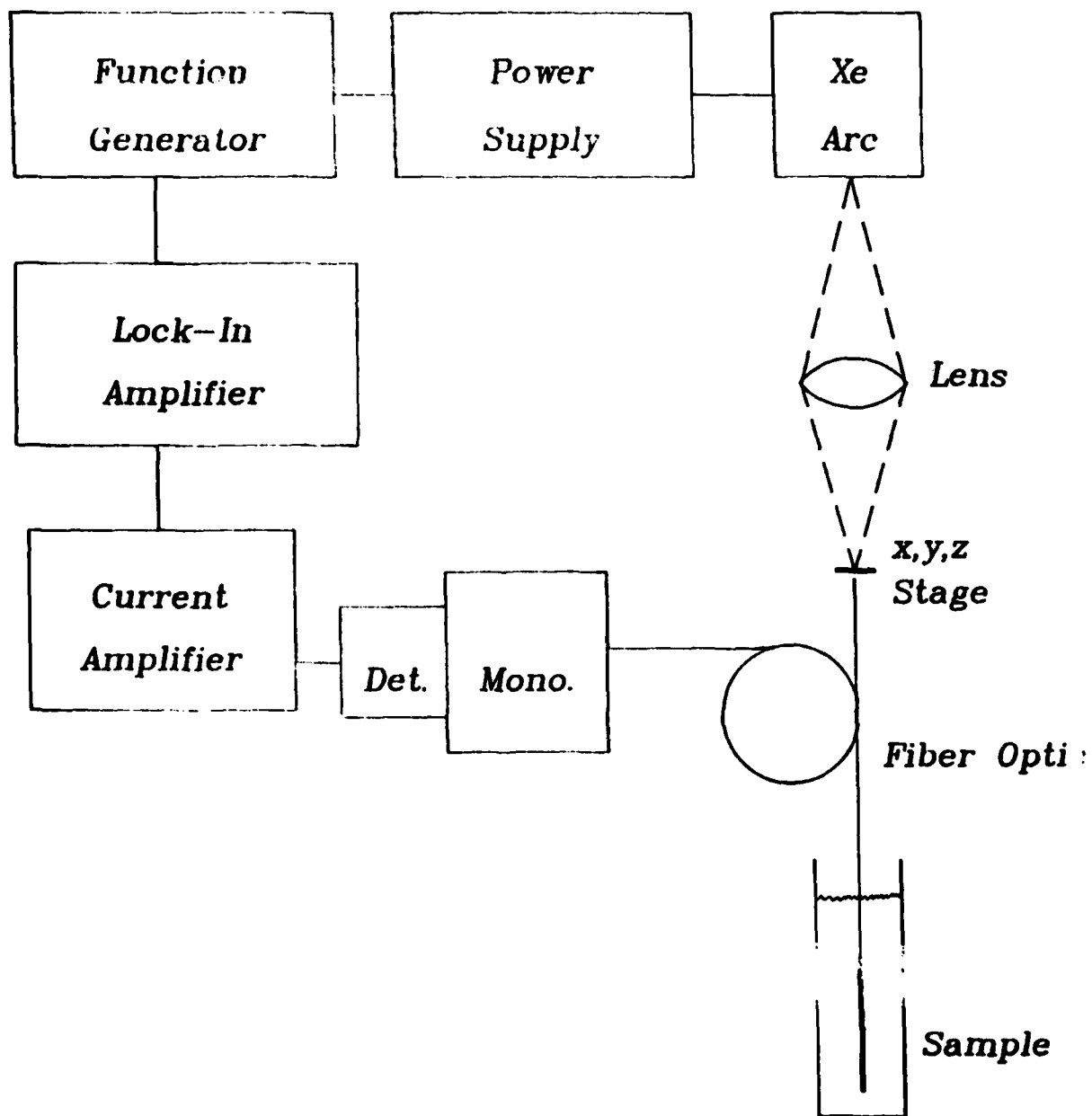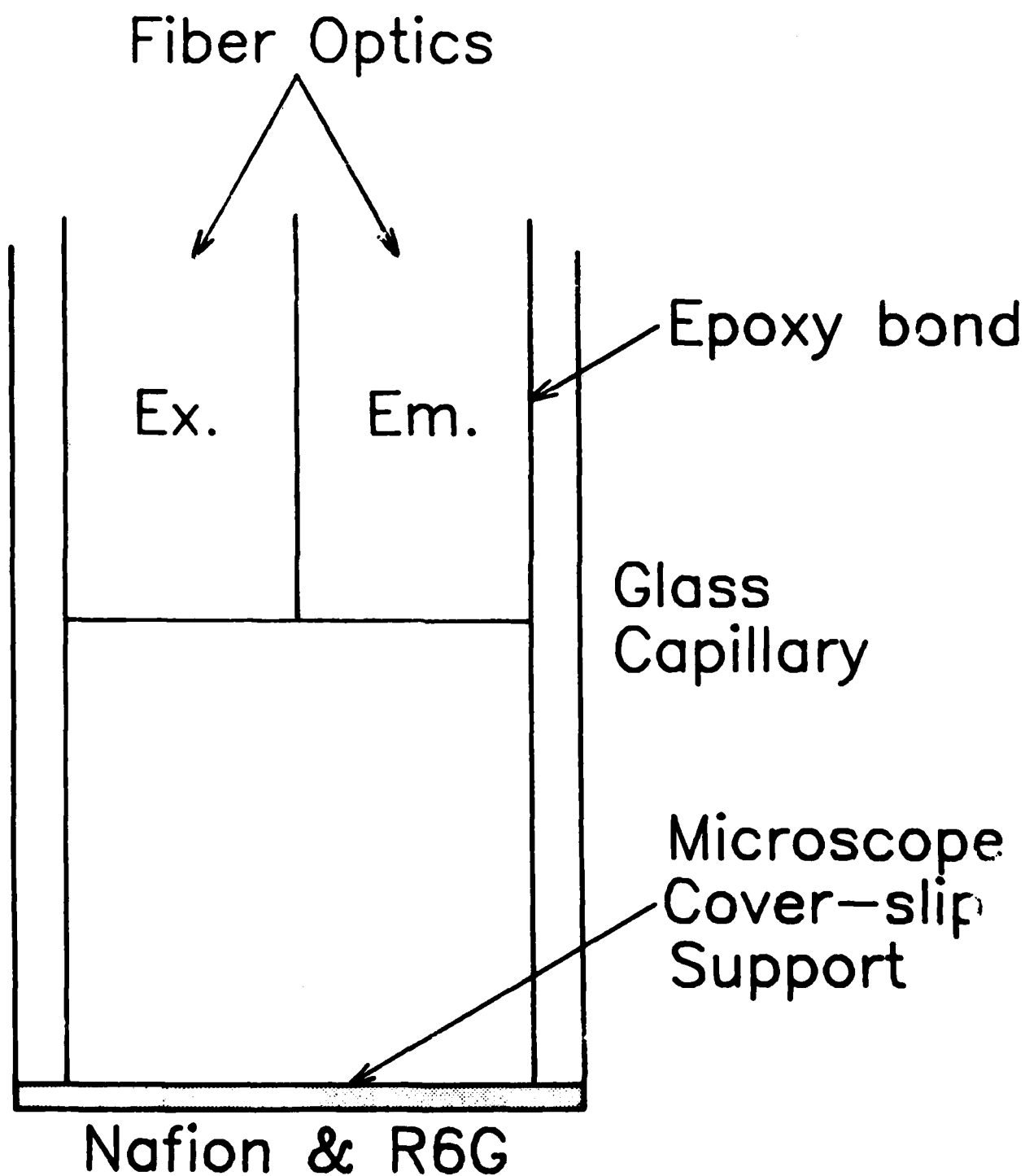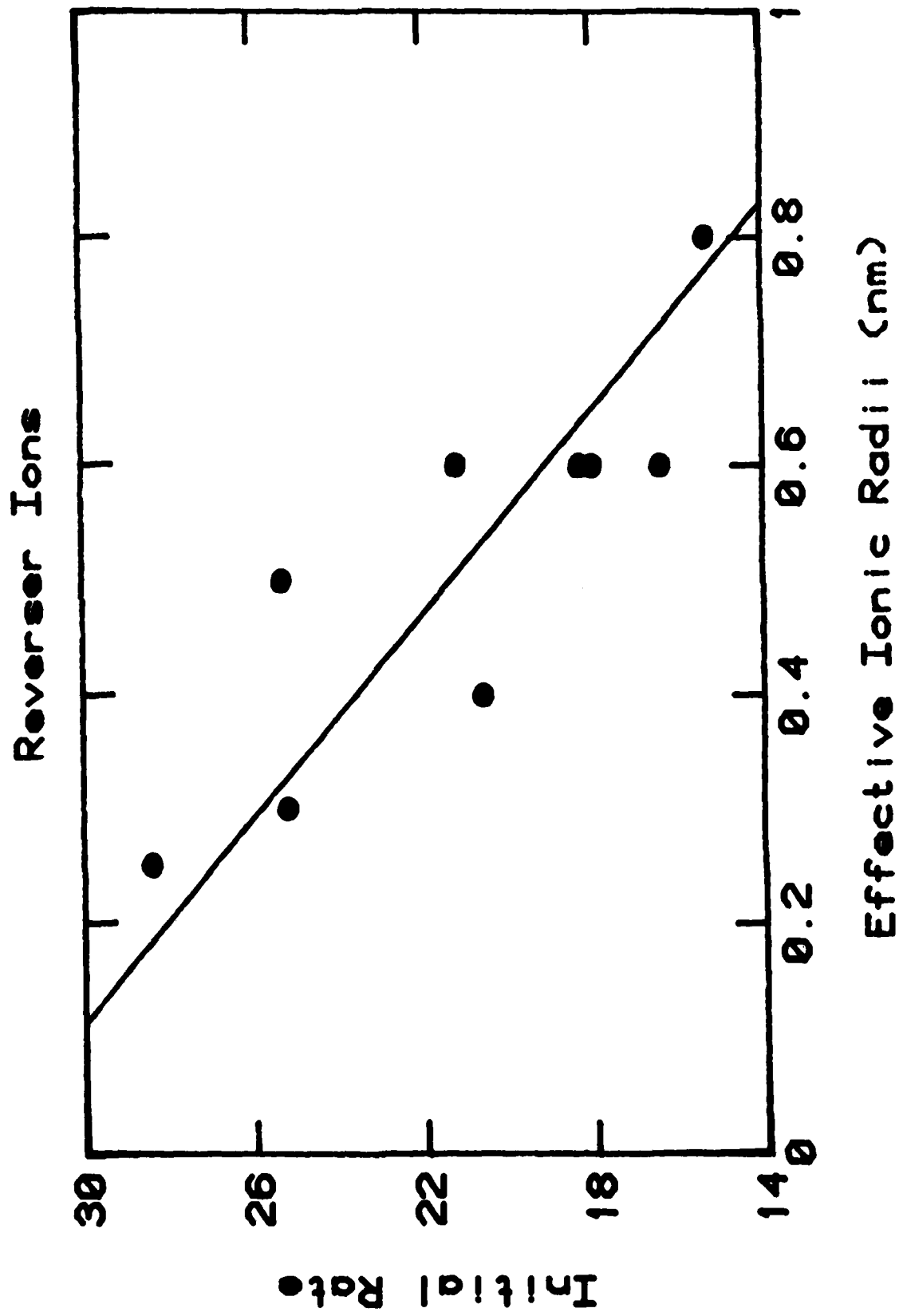
TECHNICAL REPORT DISTRIBUTION LIST, GEN

	No. Copies		No. Copies
Office of Naval Research Attn: Code 1113 800 N. Quincy Street Arlington, Virginia 22217-5000	2	Dr. David Young Code 334 NORDA NSTL, Mississippi 39529	1
Dr. Bernard Douda Naval Weapons Support Center Code 50C Crane, Indiana 47522-5050	1	Naval Weapons Center Attn: Dr. Ron Atkins Chemistry Division China Lake, California 93555	1
Naval Civil Engineering Laboratory Attn: Dr. R. W. Drisko, Code L52 Port Hueneme, California 93401	1	Scientific Advisor Commandant of the Marine Corps Code RD-1 Washington, D.C. 20380	1
Defense Technical Information Center Building 5, Cameron Station Alexandria, Virginia 22314	12 high quality	U.S. Army Research Office Attn: CRD-AA-IP P.O. Box 12211 Research Triangle Park, NC 27709	1
DTNSRDC Attn: Dr. H. Singerman Applied Chemistry Division Annapolis, Maryland 21401	1	Mr. John Boyle Materials Branch Naval Ship Engineering Center Philadelphia, Pennsylvania 19112	1
Dr. William Tolles Superintendent Chemistry Division, Code 6100 Naval Research Laboratory Washington, D.C. 20375-5000	1	Naval Ocean Systems Center Attn: Dr. S. Yamamoto Marine Sciences Division San Diego, California 91232	1

END

DATE
FILMED
5-88
DTIC